*Advances in Brief*

# Validation of the Pharmacodynamics of BMS-247550, an Analogue of Epothilone B, during a Phase I Clinical Study[1]

**Hayley M. McDaid,[2] Sridhar Mani,[2] Heng-Jia Shen, Franco Muggia, Daryl Sonnichsen, and Susan Band Horwitz[3]**

Departments of Molecular Pharmacology [H. M. D., H-J. S., S. B. H.] and Medicine [S. M.], Albert Einstein College of Medicine, Bronx, New York 10461; Albert Einstein Comprehensive Cancer Center, Bronx, New York 10461 [S. M., S. B. H.]; New York University Comprehensive Cancer Center, New York University School of Medicine, New York, New York 10016 [F. M.]; and Bristol-Myers Squibb, Wallingford, Connecticut 06492 [D. S.]

## Abstract

**The primary aims of this study were to evaluate the time course and dose response of microtubule bundle formation in peripheral blood mononuclear cells (PBMCs) and to correlate these data with BMS-247550 pharmacokinetics. The data presented here were obtained from 17 patients enrolled in a Phase I trial who received five dose levels of BMS-247550 (7.4–59.2 mg/m$^2$), given as a 1-h infusion once every 3 weeks. Plasma drug exposure or area under the curve (AUC), and tubulin bundle formation in PBMCs were assessed in cycles 1 and 2. Similar analyses were also performed on tumor biopsies from one eligible patient. PBMCs exhibited dramatic microtubule bundle formation 1 h after infusion that declined by 24 h, showing a positive correlation with $AUC_{(0-24)}$ for cycles 1 and 2. A similar pattern of tubulin bundle formation also was observed in a smaller proportion of breast tumor cells from one patient who exhibited a partial response to BMS-247550. This patient's tumor expressed multidrug resistance (MDR1) and MDR-associated protein (MRP1), and in addition poly(ADP-ribose) polymerase cleavage, a marker of cell death, was observed within 23 h after drug infusion. This patient was also heterozygous for a novel polymorphism at the extreme COOH terminus of β-tubulin (Gly 437 Gly/Ser), although the relevance of the polymorphism to the response is unknown. In summary, microtubule bundle formation in PBMCs occurs within 1 h of treatment with BMS-247550 and is related to plasma AUC. Similar bundle formation was seen in one tumor sample, despite expression of MDR1 and MRP1. Cell death occurred 23 h after peak microtubule bundle formation in these tumor cells. These findings validate *in vitro* pharmacodynamic observations.**

## Introduction

Tubulin and its polymerized form, the microtubule, are legitimate chemotherapeutic targets. Numerous small molecules bind to tubulin inducing either depolymerization of the polymer (*e.g., Vinca* alkaloids), or the polymerization of stable microtubules (*e.g.,* taxanes). Typically, these drugs induce mitotic arrest and abrogate normal microtubule dynamics, effects that eventually result in cell death. Taxol has demonstrated activity, often in combination with other agents, in the treatment and palliation of several solid tumor types, including ovarian, breast, lung, and head and neck cancers.

However, a number of disease types are inherently resistant to Taxol, notably gastrointestinal tumors and melanomas, thereby limiting the therapeutic applications for the drug. Ultimately, the majority of patients acquire resistance to Taxol, which may be mediated by a number of putative mechanisms. These include mutations in β-tubulin that have been documented in cell lines cultured *in vitro* (1, 2) and also in human tumors (3, 4). Other mechanisms of drug resistance include overexpression of the MDR[4] gene product, MDR1 (5), alterations in β-tubulin isotype expression levels (6), aberrant signal transduction pathways (7, 8) and/or apoptotic regulating proteins (9), and alterations in levels of endogenous regulators of microtubule dynamics, such as stathmin (10). It is likely that in human tumors, clinical resistance is multifactorial. The problems related to drug resistance have motivated a search for novel antimitotic agents that improve the taxane prototype by demonstrating activity in a broad spectrum of tumor types, including taxane-refractory tumors, and have a reduced propensity for acquired clinical resistance as well as having manageable toxicities, thus yielding an enhanced duration of response.

Preclinical evaluations have indicated that the epothilones are promising candidates with respect to these criteria (11). The appealing properties of the epothilones include their greater water solubility compared with Taxol and their ability to retain efficacy in cell lines expressing the MDR1 phenotype. The epothilones were originally isolated from the fermentation broth of the soil-derived myxobacterium, *Sorangium cellulosum*. The drug can be mass produced by bacterial fermentation or, more recently, by cloning of the gene cluster responsible for biosyn-

Received 12/21/01; revised 3/18/02; accepted 4/5/02.
The costs of publication of this article were defrayed in part by the payment of page charges. This article must therefore be hereby marked *advertisement* in accordance with 18 U.S.C. Section 1734 solely to indicate this fact.
[1] This study was supported by National Cancer Institute Grants U01 CA76642-01 and GCRC MOI RR00096 (to F. M.) and R03 CA86807, CA39821, and CA77263 (to S. B. H.). H. M. D. is supported by Postdoctoral Fellowship 99-3064 from the Susan G. Komen Foundation.
[2] These authors contributed equally to this work.
[3] To whom requests for reprints should be addressed, at Department of Molecular Pharmacology, Golding 201, 1300 Morris Park Avenue, Bronx, NY 10461. Phone: (718) 430-2163; Fax: (718) 430-8959; E-mail: shorwitz@aecom.yu.edu.

[4] The abbreviations used are: MDR, multidrug resistance; MRP, MDR-associated protein; PBMC, peripheral blood mononuclear cell; AUC, area under the curve (plasma drug exposure); CLT, clearance; PARP, poly(ADP-ribose) polymerase; NAT, *N*-acetyltransferase.

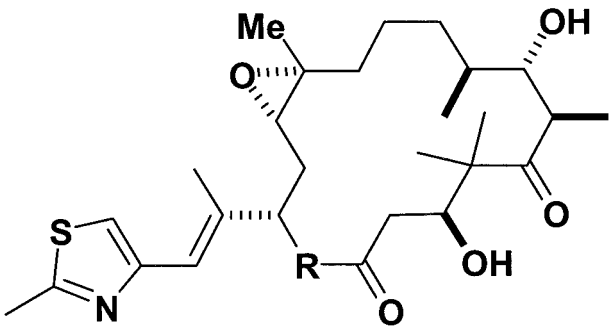


Epothilone B **R**=O

BMS-247550 **R**=N

*Fig. 1* Chemical structures of epothilone B and BMS-247550.

thesis of epothilone followed by its expression in *Streptomyces* (12). Despite these encouraging properties, the *in vivo* activities of the epothilones in animal models of human cancers were modest with a narrow therapeutic window (13). A metabolically more stable epothilone B derivative, BMS-247550, a semisynthetic lactam analogue, was designed and synthesized (Fig. 1). BMS-247550 has demonstrated antitumor activity in a number of preclinical human tumor models, including cancer cells that are inherently resistant to Taxol (14).

These data motivated an ongoing Phase I clinical evaluation of the drug (15). The biological aims of this study were to evaluate patient specimens obtained in the Phase I study and to determine the time course and dose response of microtubule bundle formation in PBMCs after exposure to BMS-247550, using the degree of microtubule bundle formation as a marker of drug binding. The occurrence of tubulin mutations/polymorphisms in available tumor tissue and PBMCs of patients enrolled in the trial, as well as other potential molecular mechanisms of drug sensitivity/resistance in this group of patients, were evaluated. This paper reports the findings of the mechanisms of action of BMS-247550 *in vivo* and corroborates *in vitro* data.

## Patients and Methods

**Phase I Clinical Evaluation of BMS-247550.** Patient eligibility, BMS-247550 formulation and dosing, together with patient pretreatment and follow-up studies will be presented in detail in a forthcoming study summarizing the clinical trial. All blood and tissue specimens used in this study were obtained under an institutional review board-approved protocol at The Albert Einstein College of Medicine.

**Pharmacokinetic Sampling.** The plasma pharmacokinetics of BMS-247550 were determined by collecting blood samples at 0 (predose), 0.5, 1 (end of infusion), 1.25, 1.5, 1.75, 2, 3, 4, 6, 8, 24, 48, and 72 h during cycles 1 and 2 for all patients. Blood was collected into labeled Vacutainer CPT Cell Preparation Tubes (Becton Dickinson, Lincoln Park, NJ) that are used to separate mononuclear cells from whole blood. Samples were centrifuged at 2500 rpm (~1000 × *g*) for 30 min at room temperature within 1 h after collection. The PBMCs and platelets that migrate as a whitish layer below the plasma were retained for subsequent tubulin bundle formation analysis (at 0-, 1-, and 24-h time points during cycles 1 and 2). In addition, purified PBMCs were stored as frozen dry pellets at −80°C for subsequent sequence analysis of class I β-tubulin. Plasma samples were transferred to labeled tubes and stored at −80°C before shipping on dry ice to the analysis site. The methods (16) used for the pharmacokinetic analysis of BMS-247550 will be described in a subsequent report.

$AUC_{(0-24)}$s were generated from peak plasma concentrations for each patient at the various pharmacokinetic sampling time points using GraphPad Prism 3.0 (GraphPad Software, Inc., San Diego, CA), in AUC mode. Correlative studies of pharmacokinetic parameters [$AUC_{(0-24)}$ and $CLT_{(0-24)}$] with the percentage of PBMCs exhibiting microtubule bundle formation were analyzed using linear regression modes.

**Tumor Biopsy Acquisition.** Biopsy specimens were obtained at 0, 1, and 24 h after BMS-247550 treatment in one patient with an accessible tumor, wherein sample acquisition involved a noninvasive procedure that required only local anesthesia. Slides for immunofluorescence were immediately prepared from tumor biopsies by imprinting the cut tumor surface onto labeled Superfrost plus slides (Fisherbrand; Fisher Scientific, Pittsburgh, PA). The slides were air dried and fixed in 100% methanol for 5 min at −20°C, after which slides were air dried and stored at 4°C. The residual tumor biopsies were immersed in 5× volumes of RNA Later (Ambion, TX) and stored at 4°C overnight to preserve endogenous nucleic acids. After refrigeration, biopsies were transferred to labeled cryostat tubes and stored at −80°C. Sections of tumor were also taken for standard histological examination (H&E staining). When required, patients submitted buccal washings for molecular analysis by rinsing briefly in water, then swirling ~5 ml of water in the mouth for ~2 min. The buccal washings were decanted into a sterile tube and centrifuged to pellet the cells that were washed with 0.5 ml of 5% FBS in PBS. The washed buccal cells were immersed in 5× volumes of RNA Later and stored at 4°C overnight to preserve endogenous nucleic acids and then stored as dry pellets at −80°C, or the total RNA was extracted immediately after recovery of the cells.

**Preparation of Cytospins.** PBMC pellets were washed twice with 0.5 ml of 5% FBS in PBS containing 0.02% $NaN_3$. The washed PBMCs were gently resuspended in 0.5 ml of 5% FBS in PBS, and the cell number was determined from ~0.1 to 0.2 ml of this cell suspension using a Coulter counter (Coulter Electronics Inc., Hialeah, FL). Glass slides (Fisherbrand) were prewet by pipetting 50 μl of 5% FBS/PBS into cytofunnels (ThermoShandon, Inc., Pittsburgh, PA) and centrifuging at maximum speed for 5 min in a cytospin (ThermoShandon, Inc.). One hundred μl of PBMC cell suspension containing approximately $0.75 \times 10^6$ cells/ml were added to cytofunnels and centrifuged at 1000 rpm for 10 min and then allowed to air dry. The slides were fixed in 100% methanol for 5–10 min at −20°C, air dried, and stored at 4°C.

**Immunohistochemistry.** Slides were rehydrated, and cells were blocked in 10% normal goat serum (Vector Labora-

tories Inc., Burlingame, CA) in PBS for 20 min at room temperature and then incubated with a 1:100 dilution of α-tubulin monoclonal antibody (Sigma Chemical Co., St. Louis, MO) diluted in 5% normal goat serum in PBS for 1 h at 37°C. The slides were rinsed in PBS and incubated with Cy3-conjugated goat antimouse IgG (1:200; Amersham, Arlington Heights, IL) for 1 h in the dark before mounting in Vectashield solution (Vector). To evaluate the degree of cell death, slides were stained with a polyclonal anti-PARP p85 antibody (Promega Corp., Madison, WI) at a dilution of 1:500, followed by a 1:200 dilution of Alexa 488 goat-antirabbit secondary antibody (Molecular Probes, OR) and mounted as described above. Slides were visualized and digitized on an Olympus IX70 inverted microscope, and cell numbers were quantified using a Zeiss Axioscop microscope. At least 500 cells/slide were counted, and the number of cells exhibiting tubulin bundle formation, or PARP positivity, was expressed as a percentage of the total number of cells counted. Samples were blinded and counted by two individual investigators to determine the mean value.

**β-Tubulin Sequence Analysis.** Tumor biopsies were homogenized (Ultra-turrax T8; IKA Laboratories) according to the RNeasy isolation method (Qiagen, Inc., Chatsworth, CA) yielding DNA-free total RNA. PBMCs and buccal cells were immersed in lysis buffer and homogenized manually. Approximately 1–2 μg of total RNA were reverse transcribed in a 50-μl reaction volume containing 300 units of Moloney murine leukemia virus reverse transcriptase (Life Technologies, Inc., Grand Island, NY) in the presence of random hexamers at a final concentration of 3.3 ng/μl, 60 units of RNAguard (Pharmacia Biotech), 0.5 mM deoxynucleotide triphosphates, 10 mM DTT, and 1× reverse transcriptase buffer at 37°C for 1 h. Samples were incubated at 95°C for 5 min and diluted 1:2 with DNase/RNase free water. Samples were aliquoted and stored at −70°C. Sequence-specific primers that span the coding region of the class I β-tubulin were designed in our laboratory and used to amplify the gene. Approximately 1 μl of cDNA was amplified in a reaction mix using 2.5 μl of 10× buffer, 2 μl of 2.5 mM $MgCl_2$, 125 ng of forward and reverse primers, and 1 unit of proofreading Taq. The PCR products were purified using the Qiaquick gel extraction kit (Qiagen), and the samples were sequenced (Genwiz, Inc., New York, NY) using the same primers as the PCR amplification. Nucleotide analysis was performed using the software Sequencher (Gene Codes Corp., Ann Arbor, MI), and the sequences were compared with the GenBank sequence for class I β-tubulin (accession number J00314).

**Reverse Transcription-PCR.** For the determination of MDR1 expression, a competitive PCR reaction using $\beta_2$-microglobulin was performed as described previously (6). MRP1 expression levels were also determined using sequence-specific primers for both genes as described previously (17). The expected PCR product size for MRP1 was 165 bp. Each experiment was performed three times.

## Results

### Clinical Endpoints ( $n = 17$)

A Phase I/II study of BMS-247550 as a 1-h infusion administered every 3 weeks is ongoing, and the maximum tolerated dose has been established in patients who received prior taxane-based chemotherapy (15). The Phase I study, as well as pharmacokinetic-pharmacodynamic relationships, will be presented subsequently. This study presented here will summarize key findings relevant to the description of molecular determinants of drug response, based on the data obtained from 17 patients enrolled in the trial. Of the patients included in this analysis, 100% had prior taxane-based chemotherapy, and >90% had either a breast or gynecological malignancy.

### Microtubule Bundle Formation in PBMCs as a Marker of BMS-247550 Pharmacodynamics

The extent of bundle formation in PBMCs was assessed in all patients as a surrogate marker of BMS-247550 binding to tubulin. Microtubule bundle formation in interphase cells is a hallmark of microtubule-stabilizing agents, such as Taxol, and is a well-documented phenomenon (5, 18). The tubulin morphology of PBMCs before and after BMS-247550 drug infusion at the 50 mg/m$^2$ dose for cycle 2 is illustrated in Fig. 2*A*. There was no bundle formation observed in PBMCs at baseline. The mean percentages of PBMCs exhibiting microtubule bundle formation at the 1- and 24-h time points were approximately 70 and 25%, respectively. The majority of PBMCs at 24 h (~75%) appeared to have normal microtubule morphology, whereas the minority (~25%) exhibited bundle formation. Fig. 3 illustrates the dose-dependent effect of BMS-247550 on microtubule bundle formation in PBMCs during cycle 1 (Fig. 3*A*) and cycle 2 (Fig. 3*B*) of treatment. Similar to the plasma pharmacokinetics of BMS-247550 (19), the degree of microtubule bundle formation in PBMCs increased to a maximum 1 h after drug infusion and then decreased by 24 h after drug infusion. This pattern was observed for all doses evaluated, except for 7.4 mg/m$^2$, a dose at which microtubule bundle formation was not detected. At the 50 mg/m$^2$ dose, where unacceptable dose-limiting toxicity was observed (15), 68–70% of PBMCs exhibited microtubule bundle formation at 1 h after infusion for cycles 1 and 2, whereas 25–28% of PBMCs exhibited the same effect at 24 h. At the 40 mg/m$^2$ dose, the values were 63% and 16–23% for 1 and 24 h after drug infusion, respectively. The pattern of bundle formation, like the pharmacokinetics of BMS-247550, was similar across cycles 1 and 2 (Fig. 3*C*), suggesting that drug binding to tubulin in PBMCs was similar across cycles 1 and 2, and that the PBMCs affected by bundle formation in cycle 1 either died or recovered by cycle 2.

To endorse these initial observations, the degree of bundle formation in PBMCs was correlated with AUC [$AUC_{(0-24)}$] (Fig. 4) and clearance [$CLT_{(0-24)}$] (Fig. 5). Because of the incomplete sampling of blood in some patients, these data were not available for all subjects. There was a positive correlation between the degree of microtubule bundle formation in PBMCs and the $AUC_{(0-24)}$ of BMS-247550 for both cycles 1 and 2 at 1 h (Fig. 4). Equally, there was a negative correlation between $CLT_{(0-24)}$ and the degree of microtubule bundle formation in PBMCs in cycles 1 and 2 at 1 h (Fig. 5, *A* and *B*, respectively). The relationship between microtubule bundle formation in PBMCs and both $AUC_{(0-24)}$ and $CLT_{(0-24)}$ at 24 h was poor. Therefore, these data indicate that the extent of microtubule bundle formation in PBMCs is related to plasma drug exposure (AUC) at 1 h after drug infusion.

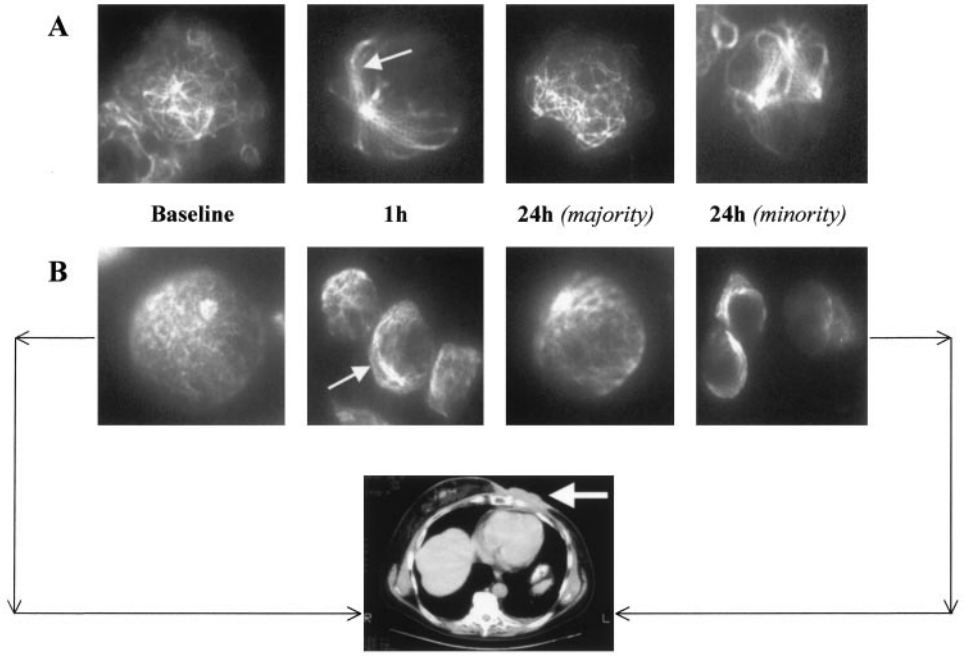


*Fig. 2* Reorganization of microtubules and bundle formation (*arrows*) before and after BMS-247550 infusion at cycle 2 (1 and 24 h) in PBMCs (*A*) and tumor (*B*) of a patient treated at the 50 mg/m$^2$ dose. At 24 h after infusion, the majority (~75%) of PBMCs had tubulin morphology that resembled baseline. ×90 Tumor biopsies were obtained at the various times from the chest wall mass, depicted in the CT scan.

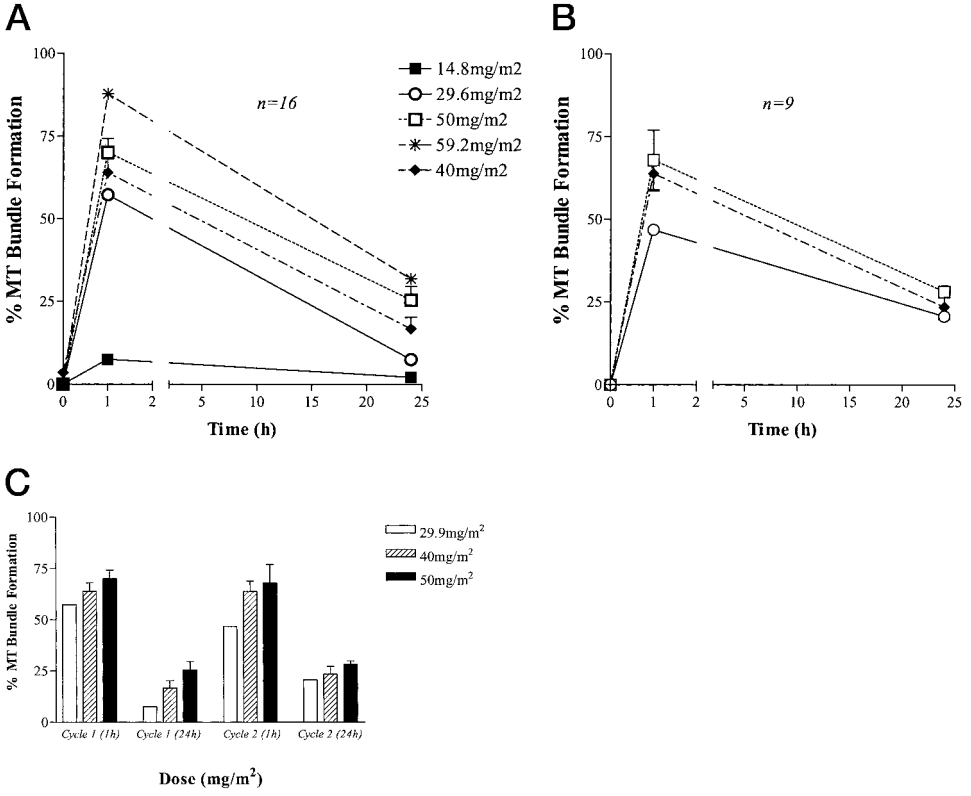


*Fig. 3* Dose- and time-dependent effects of BMS-247550 on microtubule bundle formation in PBMCs during cycle 1 (*A*) and cycle 2 (*B*) of treatment. Microtubule bundle formation, similar to pharmacokinetics, is linear across cycles 1 and 2 (*C*). Bars, SE.

**Response to BMS-247550 in Taxotere-refractory Breast Cancer: Molecular Correlates**

**Microtubule Bundle Formation and Cell Death.** One of the patients that had a partial response to BMS-247550 had an accessible chest wall mass (Fig. 2*B*), from which core biopsies were taken before and after drug infusion (1 and 24 h) in cycle 2. This patient had received prior taxotere chemotherapy and after initially responding, developed progressive disease after

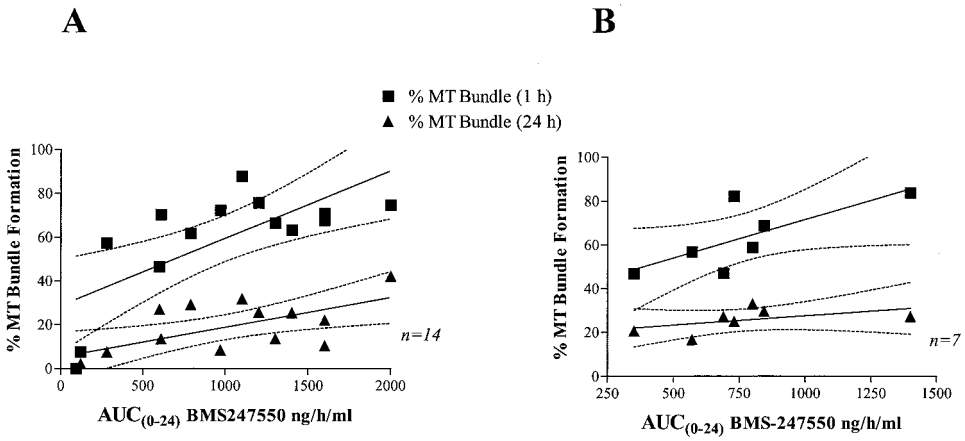


| | 1h | 24h |
|---|---|---|
| Slope: | 0.012 | 0.003 |
| $r^2$: | 0.514 | 0.415 |
| *P*: | 0.004 | 0.013 |

| | 1h | 24h |
|---|---|---|
| Slope: | 0.035 | 0.008 |
| $r^2$: | 0.550 | 0.249 |
| *P*: | 0.056 | 0.253 |

*Fig. 4* Positive correlation between percentage of microtubule bundle formation in PBMCs and $AUC_{(0-24)}$ at cycle 1 (*A*) and cycle 2 (*B*) of treatment for 1 h (■) and 24 h (▲) by linear regression analysis. *Dashed lines*, 95% confidence limits. The slopes and corresponding $r^2$ and *P*s are shown.

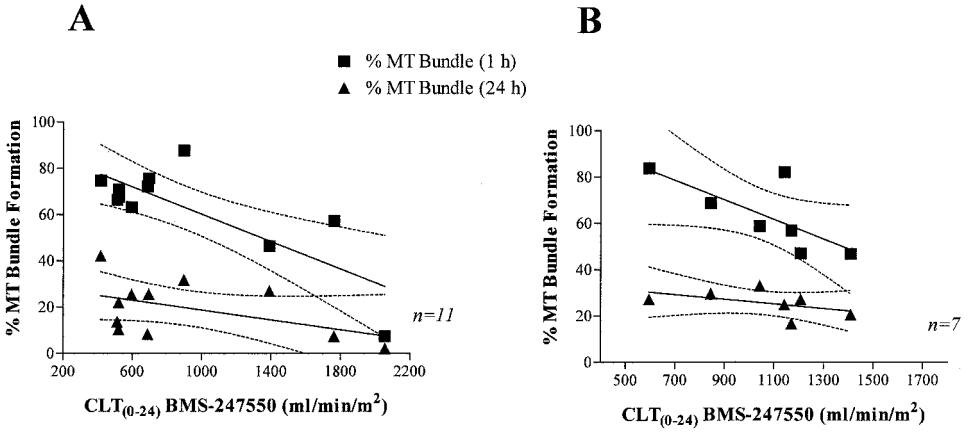


| | 1h | 24h |
|---|---|---|
| Slope: | -0.029 | -0.011 |
| $r^2$: | 0.618 | 0.242 |
| *P*: | 0.004 | 0.124 |

| | 1h | 24h |
|---|---|---|
| Slope: | -0.042 | -0.010 |
| $r^2$: | 0.542 | 0.240 |
| *P*: | 0.059 | 0.240 |

*Fig. 5* Negative correlation between the percentage of microtubule bundle formation in PBMCs and $CLT_{(0-24)}$ at cycle 1 (*A*) and cycle 2 (*B*) of treatment for 1 h (■) and 24 h (▲) by linear regression analysis. *Dashed lines*, 95% confidence limits. The slopes and corresponding $r^2$ and *P*s are shown.

~12 cycles of drug. Hence, for the purposes of this analysis, the patient was defined as taxotere refractory. This patient was treated with 50 mg/m$^2$ of BMS-247550, and a similar pattern of microtubule bundle formation was observed in the tumor cells compared with the PBMCs that were analyzed at the same cycle (Fig. 2*B*). Therefore, BMS-247550 is efficiently accrued in tumor cells within this relatively short time. No bundle formation was observed in tumor cells at baseline. The percentage of tumor cells that exhibited bundle formation were 54 ± 2% and 40 ± 4% at 1 and 24 h after drug infusion, respectively. The value for 1 h was lower than the 84 ± 4% observed in the PBMCs of the same patient at cycle 2. In contrast, the value at 24 h was higher in tumor cells than the 27 ± 5% observed in PBMCs. The difference in tumor cells compared with PBMCs at 1 and 24 h is interesting and may imply differential drug uptake and clearance kinetics, although the analyses of additional tumor biopsies after treatment will be required to validate this observation.

Because microtubule bundle formation indicates the extent of drug binding but does not provide a measure of cytotoxicity, we also evaluated the degree of PARP cleavage, a marker of cell death, in this patient's tumor cells using a highly specific antibody that recognizes only the cleaved $M_r$ 89,000 fragment of the protein. Fig. 6*A* illustrates the pattern of PARP p89 immuno-

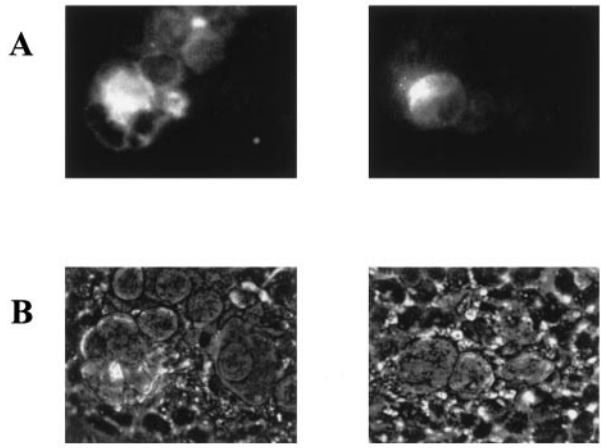


| Time | 0 h | 1 h | 24 h |
|---|---|---|---|
| % PARP positive cells | 3.4 | 3.1 | 28.2 |

*Fig. 6* PARP p89 immunostaining (*A*) and the contrasting phase images (*B*) in two representative areas of tumor, 24 h after BMS-247550 infusion (cycle 2) at the 50 mg/m$^2$ dose. 500 cells were counted to quantify the number of p89-positive cells. These data are shown for 0, 1, and 24 h. ×90.

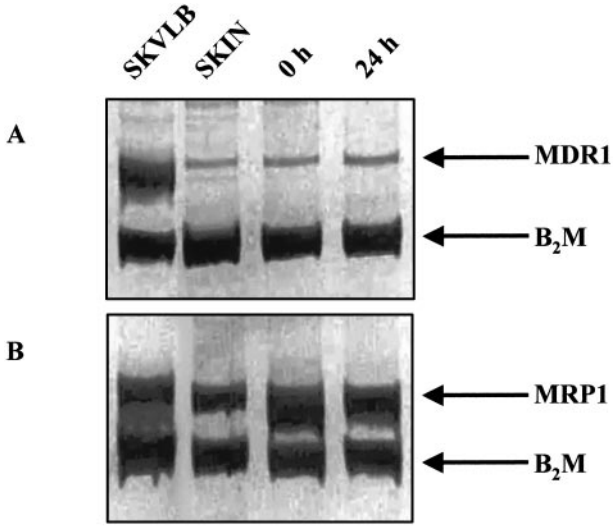


*Fig. 7* Expression of MDR1 (*A*) and MRP1 (*B*) cDNA in human ovarian SKVLB cells that overexpress both MDR1 and MRP1, in tumor biopsies (at 0 and 24 h) after treatment with BMS-247550 and in a normal skin biopsy. $\beta_2$-Microglobulin ($B_2M$) was used as a control.

staining in two representative areas of tumor, 24 h after exposure to BMS-247550. The contrasting phase images are shown in Fig. 6*B*. PARP p89 immunostaining appears to be localized to predominately nuclear regions, which is consistent with previous reports (20). The number of tumor cells exhibiting p89 staining was also quantified before and after BMS-247550. At 1 h, the number of cells exhibiting p89 staining was similar to preinfusion numbers, ~3%. At 24 h after BMS-247550 infusion, ~28% of tumor cells exhibited p89 immunostaining, indicating cytotoxic activity of BMS-247550 within 24 h after infusion. These data are consistent with the mechanism of action of chemotherapeutic agents in which cytotoxic effects occur after binding of the drug to the target. The pattern of microtubule bundle formation that we observed in these tumor cells fits this consensus, with maximum effects observed at 1 h that decreased by 24 h after infusion.

**Expression of MDR1 and MRP1.** Taxol accumulation is inhibited by the expression of MDR1, an energy-dependent drug efflux pump that maintains a low intracellular drug concentration. The role of MRP1 with respect to taxane resistance is conflicting (21, 22). We investigated the expression of both drug transporters in the tumor cells of the patient who developed progressive disease after taxotere treatment. In addition to biopsies obtained at 0, 1, and 24 h after BMS-247550, we also obtained a biopsy of normal skin, adjacent to the chest wall mass. This patient had a positive response to BMS-247550, evident after two cycles of treatment, and the chest wall mass, from which the biopsies were obtained, had a sustained regression of 5 months. The MDR1 and MRP1 status of this biopsy was also investigated. SKVLB cells that overexpress both transporters were used as a positive control. MDR1 was expressed in both the normal skin and tumor samples, but there was no up-regulation of mRNA levels in the tumor samples compared with skin or after treatment with BMS-247550 for 24 h (Fig. 7*A*). MRP1 was expressed in both the skin and tumor biopsies, and there appeared to be an overexpression of MRP1 mRNA in the tumor biopsies compared with skin (Fig. 7*B*). These data suggest that BMS-247550 retains efficacy in tumor cells expressing both MDR1 and MRP1, although more tumor samples are required to validate this preliminary finding.

**Sequence Analysis of β-Tubulin.** Increasing evidence suggests that mutations in β-tubulin may confer resistance to microtubule-interacting agents, including Taxol (23), the epothilones (1, 2), and vincristine (24). Mutations in β-tubulin also have been reported in tumor DNA isolated from the serum of patients with advanced non-small cell lung cancer (3). In light of the potential prognostic implications of these data, we sequenced the β-tubulin from the tumor biopsies obtained from one of the patients who had exhibited the partial response to BMS-247550. Sequence analysis of the cDNA and genomic DNA isolated from this patient's tumor, normal skin, PBMCs, and buccal cells indicated the presence of a novel polymorphism at the extreme COOH terminus of β-tubulin that has not been documented previously. The alteration was heterozygous: [GGT(Gly) to G/AGT(Gly/Ser)] at amino acid residue 437, present in a region of β-tubulin that is involved in its interaction with microtubule-associated proteins, motor proteins, and tau (25). The relevance of the polymorphism to the patient's response, if any, is unknown. We also analyzed the α-tubulin sequence from the tumor biopsies isolated from this patient and found no nucleotide alterations (data not shown). The remaining 16 patients were also screened for polymorphisms in β-tubulin using PBMCs as a source of nonmalignant cells. None of these patients exhibited nucleotide alterations.

## Discussion

This study of BMS-247550 in patients with advanced solid tumors describes pharmacodynamics of the drug, as well as indications of preliminary antitumor activity. The completed Phase I study will be presented in a later report. The characteristics of BMS-247550 that have been described in preclinical studies (14) have also been validated here, using molecular analyses of defined targets that potentially influence response to microtubule-stabilizing agents.

The data presented indicate that microtubule bundle formation in PBMCs is related to BMS-247550 exposure, occurs within 1 h of treatment, and correlates with the pharmacokinetics of the drug. In the context of this study, microtubule bundle formation in PBMCs is an indicator of the ability of BMS-247550 to bind to β-tubulin, and as Fig. 3 illustrates, this binding increases as the concentration of drug increases. Microtubule bundle formation is a phenotypic consequence of BMS-247550 binding to microtubules in interphase cells (5). At low drug concentrations where microtubule bundle formation is not apparent, there are still cytotoxic drug effects, presumably because of perturbations of normal microtubule dynamics (26, 27). Therefore, quantitation of microtubule bundle formation in PBMCs does not reflect intrinsic BMS-247550 activity, or the ability of this drug to produce a pharmacological effect when bound to β-tubulin, and is probably an underestimation of the number of cells that have bound BMS-247550. Despite this limitation, the preliminary data presented here suggest that microtubule bundle formation is an easily measurable, early pharmacodynamic effect.

An interesting observation that will require prospective analysis was noted with respect to the degree of microtubule bundle formation in the PBMCs of a patient who expired after one cycle of drug at the 50 mg/m$^2$ dose because of neutropenic sepsis. This patient exhibited abnormally elevated levels of bundle formation 24 h after drug infusion (42% compared with a mean of 25% ± 4 for other patients treated at this dose level). The highest percentage of bundle formation observed 24 h after infusion was 32% in a patient treated at the highest dose level of 59.2 mg/m$^2$. This patient, who exhibited high levels of bundle formation at 24 h after BMS-247550 infusion, had a CLT of 229 ml/min/m$^2$ compared with the mean value of 430 ml/min/m$^2$ for all other patients treated at this dose level, suggesting that indeed CLT was substantially lower in this patient. This suggests that higher than average levels of microtubule bundle formation in PBMCs at 24 h after BMS-247550 infusion may predict for poor clearance and may be related to subsequent toxicity.

The observation that microtubule bundle formation was reduced in the tumor cells of one patient treated at 50 mg/m$^2$ dose compared with the PBMCs at 1 h is not unexpected, because one would anticipate that drug accumulation would be highest in PBMCs that are suspended in the circulatory system. In fact, it has been demonstrated previously that the accumulation of drugs such as Taxol is reduced in multicellular spheroids, a model that closely mimics the microregions of solid tumors, compared with cells exposed to Taxol when grown in monolayers (28). Furthermore, at 24 h after infusion, the number of cells exhibiting bundle formation was higher in tumor cells compared with PBMCs (40 ± 4 compared with 27 ± 5%), suggesting that the kinetics of drug clearance may differ between the two cell types. In light of this observation, it would have been interesting to evaluate the duration of microtubule bundle formation in tumor cells; however, this was not possible because it would have required additional biopsies, although extended times for sample acquisition of both PBMCs, and tumor cells can be analyzed in prospective studies.

PARP p89 expression was chosen as a cytotoxic marker instead of the terminal deoxynucleotidyl transferase-mediated nick end labeling assay, which measures DNA strand breaks, primarily because PARP cleavage occurs before DNA strand breaks (29) and therefore is an earlier indicator of cell death. Additionally, PARP cleavage occurs during both apoptosis and necrosis (30), and we thought it prudent to measure both modes of cell death because they contribute equally to tumor regression that constitutes a clinical response. One would expect drug binding (bundle formation) to precede cell death (p89 staining), because Taxol-induced cell death is thought to be mediated via a mitochondria- regulated death pathway. Compared with classical receptor-mediated death, which occurs more quickly, activation of a mitochondria-regulated death pathway would account for the delayed time observed between bundle formation and the appearance of dead cells. The level of cell death in PBMCs was not evaluated in this study, because background levels (pre-BMS-247550) of apoptosis were high in these cells (data not shown), likely reflections of spontaneous apoptosis in mononuclear cells after collection and processing. It has been shown previously that PBMCs isolated from head and neck cancer patients undergo apoptosis more rapidly than those from persons with no evidence of cancer (31), suggesting that the lymphocytes of cancer patients may be more susceptible to apoptosis. Furthermore, apoptotic PBMCs are rapidly removed from the circulatory system by phagocytes; therefore, the quantitation of these cells undergoing apoptosis is likely to be inaccurate.

The data presented in this study document microtubule bundle formation and *in vivo* cytotoxic activity of BMS-247550 ~23 h after drug infusion in one tumor sample from a patient with taxotere-refractory metastatic breast cancer, despite expression of both drug transporters MDR1 and MRP1. These observations authenticate the preclinical data for both the epothilones and BMS-247550 (11, 14). The expression of MDR1 confers resistance to a broad spectrum of chemotherapeutic agents including the taxanes, *Vinca* alkaloids, and anthracyclines. MRP1 also mediates resistance to these drugs, although its role in taxane resistance is uncertain, and its role in the transport of epothilones has yet to be defined. MDR1 is intrinsically expressed in a number of tissue types including colon, rectum, pancreas, liver, and kidney, and its expression is induced in a number of tumor types after chemotherapy. MRP1 is expressed in epithelial cells of most normal tissues and is overexpressed in leukemia, neuroblastoma, and non-small cell lung cancer. There have been various clinical trials involving modulators of both of these drug transporters as a means of enhancing chemotherapeutic efficacy; however, a number of these modulators interact with the drugs, altering their pharmacokinetic profiles, and are therefore undesirable (32). A more acceptable means of circumventing this type of resistance is to use drugs whose transport is

minimally affected by MDR1, such as the epothilones. The findings presented here, although preliminary, are encouraging in that they confirm the expression of both MDR1 and MRP1 in the tumor of a patient who responded to BMS-247550. Furthermore, responses to epothilone B have been observed in patients with advanced colorectal cancer in a Phase I clinical evaluation (33), suggesting that this class of drug has the potential to exert cytotoxic effects in tumors that may be resistant to taxane-based chemotherapy by virtue of endogenous expression of MDR1.

A unique polymorphism was expressed in the β-tubulin of one patient, although the relevance of this polymorphism to the patient's response is unknown. This alteration was located at amino acid residue 437 of class I β-tubulin, a region of the protein that is crucial for interactions with microtubule-associated proteins, tau, and motor proteins. Although this polymorphism has not been documented previously, epothilone-resistant HeLa cells that have a heterozygous mutation at amino acid residue 422, also in the COOH terminus of class I β-tubulin, have been described (1). Attempts to increase the concentration of epothilone in which the cells were grown did not result in a more resistant phenotype with a homozygous mutation. This suggests that alterations in the COOH terminus of β-tubulin may result in severe perturbations of normal microtubule function, causing lethality. Future studies will determine whether this and other polymorphisms are expressed at the protein level and their incidence in human tumors and tissue.

The concept of genetic polymorphisms influencing drug response is not novel and constitutes an important reason for interpatient variability in chemotherapy. Examples include NAT (34), an enzyme that catalyzes the acetylation of a variety of amines. Polymorphisms have been identified in an isoform of NAT, NAT2, that were determined to mediate toxicity to amonafide, an anticancer agent that exhibited activity in breast cancer and leukemia. Amonifide is no longer in clinical development because of the potentially harmful impact of polymorphisms in NAT2. Likewise, there are polymorphisms that positively influence tumor response (35); therefore, the possibility exists that polymorphisms in class I β-tubulin may modulate response to drugs that bind to this target, including the taxanes and epothilones. This hypothesis will require validation, but the outcome may benefit patients who will be treated with this class of drug.

## Acknowledgments

We gratefully acknowledge Drs. Susan Arbuck, Dimitrios Colevas, Abbey Fields, Susan Galbraith, Louise Grochow, Anne Hamilton, Howard Hochster, David Lebwohl, Leonard Liebes, Carolyn Runowicz, and Joseph Sporano for help with this study.

## References

1. He, L., Yang, C-P. H., and Horwitz, S. B. Mutations in β-tubulin map to domains involved in regulation of microtubule stability in epothilone-resistant Cell Lines. Mol. Cancer Therapeut., *1:* 1–8, 2001.

2. Giannakakou, P., Gussio, R., Nogales, E., Downing, K. H., Zaharevitz, D., Bollbuck, B., Poy, G., Sackett, D., Nicolaou, K. C., and Fojo, T. A common pharmacophore for epothilone and taxanes: molecular basis for drug resistance conferred by tubulin mutations in human cancer cells. Proc. Natl. Acad. Sci. USA, *97:* 2904–2909, 2000.

3. Monzo, M., Rosell, R., Sanchez, J. J., Lee, J. S., O'Brate, A., Gonzalez-Larriba, J. L., Alberola, V., Lorenzo, J. C., Nunez, L., Ro, J. Y., and Martin, C. Paclitaxel resistance in non-small-cell lung cancer associated with β-tubulin gene mutations. J. Clin. Oncol., *17:* 1786–1793, 1999.

4. Rosell, R., Monzo, M., Gandara, D., Gumerlock, P., Font, A., and Taron, M. Development of a docetaxel-based trial in non-small-cell lung cancer based on presence of β-tubulin mutations. Adv. Lung Cancer, *3:* 2–5, 2001.

5. Horwitz, S. B., Cohen, D., Rao, S., Ringel, I., Shen, H. J., and Yang, C. P. Taxol: mechanisms of action and resistance. J. Natl. Cancer Inst. Monogr., *15:* 55–61, 1993.

6. Kavallaris, M., Kuo, D. Y., Burkhart, C. A., Regl, D. L., Norris, M. D., Haber, M., and Horwitz, S. B. Taxol-resistant epithelial ovarian tumors are associated with altered expression of specific β-tubulin isotypes. J. Clin. Investig., *100:* 1282–1293, 1997.

7. Yu, D., Liu, B., Jing, T., Sun, D., Price, J. E., Singletary, S. E., Ibrahim, N., Hortobagyi, G. N., and Hung, M. C. Overexpression of both p185c-erbB2 and p170mdr-1 renders breast cancer cells highly resistant to Taxol. Oncogene, *16:* 2087–2094, 1998.

8. Montgomery, R. B., Guzman, J., O'Rourke, D. M., and Stahl, W. L. Expression of oncogenic epidermal growth factor receptor family kinases induces paclitaxel resistance and alters β-tubulin isotype expression. J. Biol. Chem., *275:* 17358–17363, 2000.

9. Strobel, T., Tai, Y. T., Korsmeyer, S., and Cannistra, S. A. BAD partly reverses paclitaxel resistance in human ovarian cancer cells. Oncogene, *17:* 2419–2427, 1998.

10. Iancu, C., Mistry, S. J., Arkin, S., and Atweh, G. F. Taxol and anti-stathmin therapy: a synergistic combination that targets the mitotic spindle. Cancer Res., *60:* 3537–3541, 2000.

11. Bollag, D. M., McQueney, P. A., Zhu, J., Hensens, O., Koupal, L., Liesch, J., Goetz, M., Lazarides, E., and Woods, C. M. Epothilones, a new class of microtubule-stabilizing agents with a Taxol-like mechanism of action. Cancer Res., *55:* 2325–2333, 1995.

12. Tang, L., Shah, S., Chung, L., Carney, J., Katz, L., Khosla, C., and Julien, B. Cloning and heterologous expression of the epothilone gene cluster. Science (Wash. DC), *287:* 640–642, 2000.

13. Chou, T. C., Zhang, X. G., Balog, A., Su, D. S., Meng, D., Savin, K., Bertino, J. R., and Danishefsky, S. J. Desoxyepothilone B: an efficacious microtubule-targeted antitumor agent with a promising *in vivo* profile relative to epothilone B. Proc. Natl. Acad. Sci. USA, *95:* 9642–9647, 1998.

14. Lee, F. Y., Borzilleri, R., Fairchild, C. R., Kim, S. H., Long, B. H., Reventos-Suarez, C., Vite, G. D., Rose, W. C., and Kramer, R. A. BMS-247550: a novel epothilone analog with a mode of action similar to paclitaxel but possessing superior antitumor efficacy. Clin. Cancer Res., *7:* 1429–1437, 2001.

15. Mani, S., McDaid, H. M., Shen, H. J., Sporano, A., Hamilton, C., Runowicz, H., Hochester, H., Muggia, F., Fields, A., Damle, B., Letrent, S., Lebwohl, D., and Horwitz, S. B. Phase I Evaluation of an epothilone B analog (BMS-247550): clinical findings and molecular correlates. Proc. Am. Soc. Clin. Oncol., *20:* 68a, 2001.

16. Lee, F. Y. F. Pharmacodynamic and Pharmacokinetic Studies to Determine the Minimum Effective Exposure of BMS-247550 Required for Antitumor Activity *in Vivo*. Bristol-Myers Squibb Pharmaceutical Research Institute, Princeton, NJ, 1999.

17. Bordow, S. B., Haber, M., Madafiglio, J., Cheung, B., Marshall, G. M., and Norris, M. D. Expression of the multidrug resistance-associated protein (*MRP*) gene correlates with amplification and overexpression of the N-*myc* oncogene in childhood neuroblastoma. Cancer Res., *54:* 5036–5040, 1994.

18. Schiff, P. B., and Horwitz, S. B. Taxol stabilizes microtubules in mouse fibroblast cells. Proc. Natl. Acad. Sci. USA, *77:* 1561–1565, 1980.

19. Damle, B. D., Letrent, S., Duncan, G., Litwin, V., Panting, L., Lebwohl, D., Jones, S., Burris, H., and Spriggs, D. Pharmacokinetics (PK) and pharmacodynamics (PD) of BMS-247550, an epothilone B analog, in patients with advanced solid tumors. Proc. Am. Soc. Clin. Oncol., *20:* abstract 268, 2001.

20. O'Brien, M. A., Moravec, R. A., and Riss, T. L. Poly(ADP-ribose) polymerase cleavage monitored *in situ* in apoptotic cells. Biotechniques, *30:* 886–891, 2001.

21. Breuninger, L. M., Paul, S., Gaughan, K., Miki, T., Chan, A., Aaronson, S. A., and Kruh, G. D. Expression of multidrug resistance-associated protein in NIH/3T3 cells confers multidrug resistance associated with increased drug efflux and altered intracellular drug distribution. Cancer Res., *55:* 5342–5347, 1995.

22. Vanhoefer, U., Cao, S., Harstrick, A., Seeber, S., and Rustum, Y. M. Comparative antitumor efficacy of docetaxel and paclitaxel in nude mice bearing human tumor xenografts that overexpress the multidrug resistance protein (MRP). Ann. Oncol., *8:* 1221–1228, 1997.

23. Giannakakou, P., Sackett, D. L., Kang, Y. K., Zhan, Z., Buters, J. T., Fojo, T., and Poruchynsky, M. S. Paclitaxel-resistant human ovarian cancer cells have mutant β-tubulins that exhibit impaired paclitaxel-driven polymerization. J. Biol. Chem., *272:* 17118–17125, 1997.

24. Kavallaris, M., Tait, A. S., Walsh, B. J., He, L., Horwitz, S. B., Norris, M. D., and Haber, M. Multiple microtubule alterations are associated with *Vinca* alkaloid resistance in human leukemia cells. Cancer Res., *61:* 5803–5809, 2001.

25. Nogales, E., Wolf, S. G., and Downing, K. H. Structure of the αβ tubulin dimer by electron crystallography. Nature (Lond.), *391:* 199–203, 1998.

26. Jordan, M. A., Toso, R. J., Thrower, D., and Wilson, L. Mechanism of mitotic block and inhibition of cell proliferation by Taxol at low concentrations. Proc. Natl. Acad. Sci. USA, *90:* 9552–9556, 1993.

27. Torres, K., and Horwitz, S. B. Mechanisms of Taxol-induced cell death are concentration dependent. Cancer Res., *58:* 3620–3626, 1998.

28. Nicholson, K. M., Bibby, M. C., and Phillips, R. M. Influence of drug exposure parameters on the activity of paclitaxel in multicellular spheroids. Eur. J. Cancer, *33:* 1291–1298, 1997.

29. Li, X., and Darzynkiewicz, Z. Cleavage of poly(ADP-ribose) polymerase measured *in situ* in individual cells: relationship to DNA fragmentation and cell cycle position during apoptosis. Exp. Cell Res., *255:* 125–132, 2000.

30. Gobeil, S., Boucher, C. C., Nadeau, D., and Poirier, G. G. Characterization of the necrotic cleavage of poly(ADP-ribose) polymerase (PARP-1): implication of lysosomal proteases. Cell Death Differ., *8:* 588–594, 2001.

31. Saito, T., Kuss, I., Dworacki, G., Gooding, W., Johnson, J. T., and Whiteside, T. L. Spontaneous *ex vivo* apoptosis of peripheral blood mononuclear cells in patients with head and neck cancer. Clin. Cancer Res., *5:* 1263–1273, 1999.

32. Peck, R. A., Hewett, J., Harding, M. W., Wang, Y. M., Chaturvedi, P. R., Bhatnagar, A., Ziessman, H., Atkins, F., and Hawkins, M. J. Phase I and pharmacokinetic study of the novel MDR1 and MRP1 inhibitor biricodar administered alone and in combination with doxorubicin. J. Clin. Oncol., *19:* 3130–3141, 2001.

33. Calvert, P. M., O'Neill, V., Twelves, C., Azzabi, A., Hughes, A., Bale, C., Robinson, A., Machan, M., Dimitrijevic, S., Moss, D., Rothermel, J., Cohen, P., Chen, T., Man, A., and Calvert, A. A Phase I clinical and pharmacokinetic study of EP0906 (epothilone B), given every three weeks, in patients with advanced solid tumors. Proc. Am. Soc. Clin. Oncol., *20:* 108a, 2001.

34. Innocenti, F., Iyer, L., and Ratain, M. J. Pharmacogenetics of anticancer agents: lessons from amonafide and irinotecan. Drug Metab. Dispos., *29:* 596–600, 2001.

35. Bamber, D. E., Fryer, A. A., Strange, R. C., Elder, J. B., Deakin, M., Rajagopal, R., Fawole, A., Gilissen, R. A., Campbell, F. C., and Coughtrie, M. W. Phenol sulphotransferase *SULT1A1*1* genotype is associated with reduced risk of colorectal cancer. Pharmacogenetics, *11:* 679–685, 2001.

Clinical Cancer Research

# Validation of the Pharmacodynamics of BMS-247550, an Analogue of Epothilone B, during a Phase I Clinical Study

Hayley M. McDaid, Sridhar Mani, Heng-Jia Shen, et al.

*Clin Cancer Res* 2002;8:2035-2043.